Self-Assembly of Stimuli-Responsive Water-Soluble [60]Fullerene End-Capped Ampholytic Block Copolymer

Soon Kay Teoh,[†,§] Palaniswamy Ravi,[†,‡] Sheng Dai,[†,‡] and Kam Chiu Tam*[,†,‡]

School of Mechanical and Aerospace Engineering and Division of Chemical and Biomolecular Engineering and Singapore-MIT Alliance, Nanyang Technological University, 50 Nanyang Avenue, Singapore 639798, Republic of Singapore

Received: October 7, 2004; In Final Form: December 22, 2004

A well-defined, water-soluble, pH and temperature stimuli-responsive [60]fullerene (C_{60}) containing ampholytic block copolymer of poly((methacrylic acid)-block-(2-(dimethylamino)ethyl methacrylate))-block-C_{60} (P(MAA-*b*-DMAEMA)-*b*-C_{60}) was synthesized by the atom transfer radical polymerization (ATRP) technique. The self-assembly behavior of the C_{60} containing polyampholyte in aqueous solution was characterized by potentiometric and conductometric titration, dynamic light scattering (DLS), and transmission electron microscopy. This amphiphilic mono-C_{60} end-capped block copolymer shows enhanced solubility in aqueous medium at room and elevated temperatures and at low and high pH but phase separates at intermediate pH between 5.4 and 8.8. The self-assembly of the copolymer is different from that of P(MAA-*b*-DMAEMA). Examination of the association behavior using DLS revealed the coexistence of unimers and aggregates at low pH at all temperatures studied, with the association being driven by the balance of hydrophobic and electrostatic interactions. Unimers and aggregates of different microstructures are also observed at high pH and at temperatures below the lower critical solution temperature (LCST) of PDMAEMA. At high pH and at temperatures above the LCST of PDMAEMA, the formation of micelles and aggregates coexisting in solution is driven by the combination of hydrophobic, electrostatic, and charge-transfer interactions.

Introduction

Despite the discovery of potential applications of fullerenes in biological systems, the insolubility of fullerenes in water and organic solvents has hindered the progress in this field of research.[1] The solubility of fullerenes can be enhanced through the formation of charge-transfer complexes with organic compounds possessing electron-donating properties[2,3] In addition, their solubility can also be enhanced by functionalizing the fullerenes with hydrophilic compounds, such as alcohols,[4] carboxylic acids,[5] amines,[6] or long-chain hydrophilic polymers.[7,8] These amphiphilic fullerene derivatives self-assemble into nanoscale structures in water, which have a variety of potential applications.[9]

To date, monosubstituted fullerenes with well-defined polymers have been synthesized and their solution behavior examined since these polymers retain the unique fullerene properties and may have potential biological applications. For example, core−shell-like micelles from PMMA-*b*-C_{60} and P*n*BMA-*b*-C_{60} systems in THF[10] and large spherical aggregates from single- and two-arm fullerene-containing poly(ethylene oxide)s in THF and aqueous solution[11,12] have been reported. Recently, Zhou and co-workers employed ATRP to synthesize well-defined fullerene-containing polystyrene and poly(methyl methacrylate).[13] Water-soluble C_{60}-containing poly(acrylic acid) (PAA-*b*-C_{60}) synthesized by Yang et al. formed core−shell micelles in aqueous solution, which enhanced the photoconductivity of film.[14] Recently, we have synthesized a series of well-defined C_{60}-containing water-soluble polymeric systems using ATRP, such as poly(methacrylic acid)-*b*-C_{60} (PMAA-*b*-C_{60}) and poly(2-(dimethylamino)ethyl methacrylate)-*b*-C_{60} (PDMAEMA-*b*-C_{60}), and their self-assembly behavior in aqueous solution was studied as a function of pH and temperature.[15,16]

Stimuli-responsive block copolymers are an interesting class of block copolymers because their physical and chemical properties can be adjusted by external stimuli. For example, hydrophilic or hydrophobic properties can be induced by the variation of pH or temperature.[17,18] This type of reversible change has far-reaching consequences on the aggregation, phase behavior, and solubility, leading to widespread applications in drug delivery systems[19] and in devices such as actuators,[20] artificial muscles,[21] and controlled molecular gates and switches.[22] Studies conducted on the stimuli-responsive drug-release behavior of block copolymers have revealed their possible applications.[23,24] Since PMAA and PDMAEMA are proven to be stimuli-responsive and biocompatible,[25,26] studies have been conducted on P(MAA-*b*-DMAEMA) block copolymers in the dilute regime as a function of pH and concentration.[27,28] The self-assembly of PAA-*b*-C_{60}, PMAA-*b*-C_{60}, and PDMAEMA-*b*-C_{60} have been studied as a function of pH. Since the polyampholytes exhibit anti-polyelectrolyte behaviors, the solution behavior of C_{60}-containg polyampholytes is unexplored. The combination of stimuli responsive amphiphilic behaviors of the polymeric segments and C_{60} makes the system more attractive as a drug delivery vehicle. It is important to understand the self-assembly behavior of P(MAA-*b*-DMAEMA)-*b*-C_{60} system in aqueous solution prior to their applications in various biomedical applications. In this paper, a well-defined ampholytic C_{60}-containing P(MAA-*b*-DMAEMA) (P(MAA-*b*-DMAEMA)-

* To whom correspondence should be addressed. Fax: (65) 67911859. E-mail: mkctam@ntu.edu.sg.

† School of Mechanical and Aerospace Engineering and Division of Chemical and Biomolecular Engineering.

‡ Singapore-MIT Alliance.

§ Present address: School of Chemical Engineering, Purdue University.

10.1021/jp045413r CCC: $30.25
Published on Web 02/18/2005

SCHEME 1: Synthetic Scheme for P(MAA$_{102}$-*b*-DMAEMA$_{67}$)-*b*-C$_{60}$

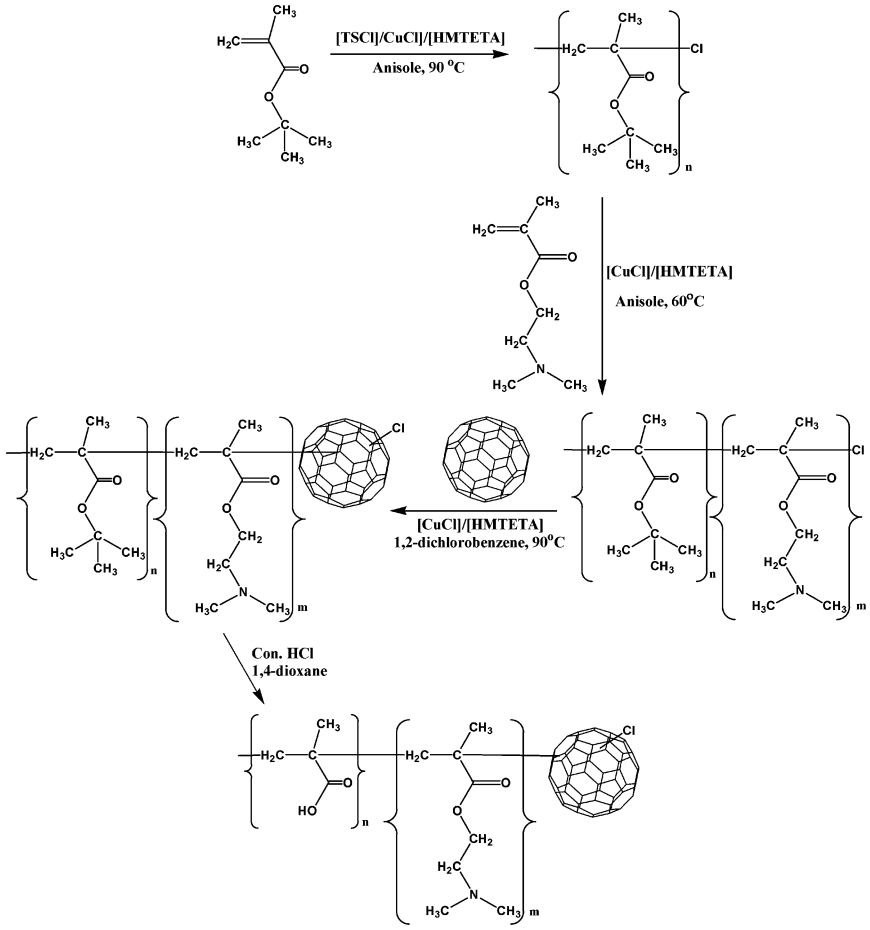

b-C$_{60}$) was synthesized using the ATRP technique, and its pH- and temperature-responsive aggregation behavior in dilute aqueous solution was examined in detail.

Experimental Procedures

Materials. C$_{60}$ (99.9%) was obtained from Materials Technologies Research (MTR) Ltd. 2-(Dimethylamino)ethyl methacrylate (DMAEMA), *t*-butyl methacrylate (*t*BMA), CuCl (99.995%), and 1,1,4,7,10,10-hexamethyltriethylenetetramine (HMTETA, 97%) were obtained from Aldrich and used without further purification. The monomers were purified by passing through a basic alumina column, dried over CaH_2, and distilled under reduced pressure. All solvents were freshly distilled before use.

Synthesis of P(*t*BMA-*b*-DMAEMA)-Cl Macroinitiator. All the synthetic steps were carried out under an argon atmosphere. First, the well-defined -Cl terminated P*t*BMA macroinitiator (M_n = 14 500 Da and M_w/M_n = 1.13) was synthesized as described in our previous paper.[9] To a Schlenk flask, a known amount of P*t*BMA-Cl, CuCl (molar equivalent to P*t*BMA), DMAEMA monomer, and anisole (1:1 volume ratio to monomer) was introduced. The reaction mixture was degassed three times using freeze−pump−thaw cycles. The degassed ligand (HMTETA, molar equivalent to P*t*BMA) was introduced just before the final cycle, and the flask was placed in a thermostated oil bath at 60 °C. When the reaction yield reached ~90%, the reaction was stopped. The catalyst was removed using a basic alumina column, and the polymer was recovered by precipitation in excess of cold *n*-hexane, filtered, and dried under vacuum. The reprecipitation process was repeated three times to remove unreacted monomers and impurities.

Synthesis of P(MAA-*b*-DMAEMA)-*b*-C$_{60}$. P(*t*BMA-*b*-DMAEMA)-Cl was charged into a Schlenk flask and dissolved in a small amount of 1,2-dichlorobenzene. In a separate Schlenk flask, C$_{60}$ (P(*t*BMA-*b*-DMAEMA)-Cl:C$_{60}$ molar ratio of 1:3) and CuCl/HMTETA (1:1) catalyst systems were dissolved in 20 mL of 1,2-dichlorobenzene. Three freeze−pump−thaw cycles were performed for both the Schlenk flasks. Finally, the macroinitiator was added into the catalyst complex via a double-tipped syringe and reacted for 24 h at 90 °C. After 24 h, the reaction mixture was diluted with THF. The catalyst was first removed using a basic alumina column, and the solvent was then evacuated under vacuum. The unreacted C$_{60}$ was removed by the polymer being dissolved in THF, filtered, and passed through the alumina column. The filtrate was concentrated and precipitated in excess amounts of cold *n*-hexane to yield a dark brown polymer. The procedure was repeated three times to ensure the complete removal of unreacted C$_{60}$. Subsequently, the *t*-butyl groups of the P(*t*BMA) blocks were hydrolyzed with concentrated hydrochloric acid in 1,4-dioxane at 85 °C for 6 h to form PMAA blocks, and the block copolymer was precipitated in excess of *n*-hexane. The polymer was washed with *n*-hexane for several times and dried under vacuum. The fully hydrolyzed final product was confirmed by FT-IR (KBr-pellet) and potentiometric titration.

Gel Permeation Chromatography. An Agilent 1100 series GPC system equipped with a LC pump, PLgel 5μm MIXED-C column, RI, and RI/UV dual mode detectors was used to determine polymer molecular weights and polydispersity. The UV/RI (330 nm was used to monitor the signal) dual detector system was used to confirm the grafting of C$_{60}$ onto the polymer. The column was calibrated with narrow molecular weight

polystyrene standards. HPLC grade THF stabilized with BHT was used as the mobile phase. The flow rate was maintained at 1.0 mL/min.

NMR Spectroscopy. The ^{1}H NMR spectrum of the precursor block copolymer was measured using a Brüker DRX400 instrument in $CDCl_3$.

Thermogravimetric Analysis. Thermogravimetric measurements were carried out with a Perkin-Elmer TGA 7 Thermogravimetric Analyzer. A fixed amount of samples were heated from 25 to 850 °C at a rate of 10 °C/min in a dynamic nitrogen atmosphere.

UV−Vis Spectroscopy. Absorption measurements were made on copolymer solutions at 25 °C with concentrations ranging from 0.025 to 0.25 wt % using an Agilent 8453 UV−vis spectrophotometer at pH 3 and 11. Visible light transmittance measurements were carried out at 25 and 55 °C with a wavelength of 600 nm on 0.3 wt % copolymer solution.

Potentiometric and Conductometric Titrations. Both titration measurements were carried out with a Radiometer ABU93 Triburet titrator on 0.05 wt % aqueous copolymer solution from pH 3 to 11 using standard NaOH titrant at 25 °C. The temperature was controlled by a PolyScience water bath.

Dynamic Light Scattering. Room-temperature light scattering measurements were made with a Brookhaven BI-200SM goniometer equipped with a BI9000AT digital correlator. Intermediate and elevated temperature light scattering measurements were made with a Brookhaven ZetaPlus system equipped with temperature control unit. The inverse Laplace transformation of REPES in the GENDIST software package was used to obtain decay time distribution functions with the probability-to-reject set at 0.5. The copolymer concentrations ranged from 0.05 to 0.30 wt % in 0.1 M NaCl solution, while the scattering angles were varied from 30 to 90°.

Transmission Electron Microscopy. For each transmission electron microscopic sample, a drop of dilute copolymer solution was placed onto a 200-mesh copper grid precoated either with carbon or Formvar. The samples were dried overnight before measurement using a JEOL JEM 2010 transmission electron microscope operating at an accelerating voltage of 200 kV.

Results and Discussion

Recently, well-defined poly(methyl methacrylate) and polystyrene have been successfully mono-end-capped with C_{60} using the ATRP technique.[13] The synthesis details for P(MAA-*b*-DMAEMA)-*b*-C_{60} are described in Scheme 1. In this study, we first synthesized a well-defined -Cl terminated P*t*BMA with M_n = 14 500 Da and M_w/M_n = 1.13,[9] as determined from the GPC trace (Figure 1a). Using the P*t*BMA-Cl as macroinitiator, DMAEMA was block copolymerized in the presence of a CuCl/HMTETA catalyst system in anisole at 60 °C. Figure 1b shows the monomodal GPC curve of P(*t*BMA-*b*-DMAEMA)-Cl. The precursor P*t*BMA macroinitiator was absent, which implies that all the end groups of P*t*BMA chains are active during the copolymerization process. This strongly supports the controlled/living character of the copolymerization. The GPC trace (Figure 1b) indicates that the copolymer possesses a M_n of 25 200 Da and M_w/M_n of 1.18. The ^{1}H NMR spectrum of the P(*t*BMA-*b*-DMAEMA) block copolymer as shown in Figure 2 allows the molar composition to be determined from the relative intensity at 1.42 ppm (−C(C**H**$_3$)$_3$ of the *t*BMA block) and 2.30 ppm (−N(C**H**$_3$)$_2$ of DMAEMA block). On the basis of the combination of ^{1}H NMR and GPC traces, the degree of polymerization was determined to be P(*t*BMA$_{102}$-*b*-DMAEMA$_{67}$).

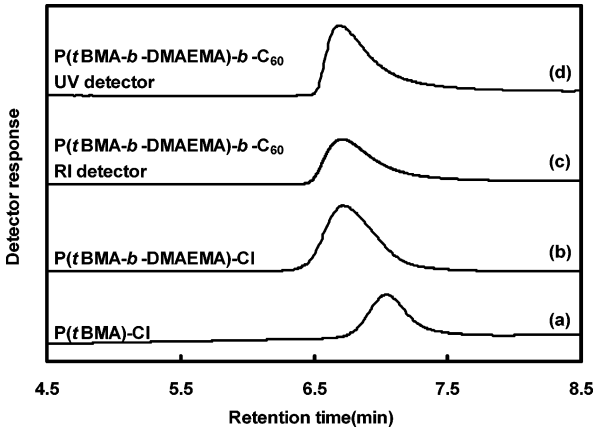

Figure 1. GPC traces of P*t*BMA-Cl (a), P(*t*BMA-*b*-DMAEMA)-Cl (b), P(*t*BMA-*b*-DMAEMA)-*b*-C_{60} (c) from RI detector, and GPC trace of P(*t*BMA-*b*-DMAEMA)-*b*-C_{60} (d) from UV detector.

Using the P(*t*BMA-*b*-DMAEMA)-Cl macroinitiator, ATRP was again used to functionalize C_{60} using the same catalyst system. The molar ratio of 1:3 (P(*t*BMA-*b*-DMAEMA)-Cl:C_{60}) was used to avoid multiple grafting of the polymer on C_{60}. The GPC traces for P(*t*BMA-*b*-DMAEMA)-*b*-C_{60} determined using different detectors (RI and RI/UV dual detectors) are compared in Figure 1c,d. The monomodal GPC trace from the RI detector revealed that the molecular weight of the P(*t*BMA-*b*-DMAEMA)-*b*-C_{60} polymer was 25 300 Da with M_w/M_n = 1.22. The small contribution of the C_{60} molecule to the hydrodynamic volume results in an insignificant increase in the molecular weight of the fullerene grafted polymer.[13] Also, the absence of any tailing or multiple peaks confirmed the monosubstitution of the copolymer onto C_{60} molecules. Since only copolymer chains with C_{60} were detectable from both UV (λ ∼330 nm) and RI detectors, the GPC traces (Figure 1d) confirmed that P(*t*BMA-*b*-DMAEMA) chains have been covalently bonded to C_{60} molecules. The GPC traces of P(*t*BMA-*b*-DMAEMA)-*b*-C_{60} detected from both UV and RI detectors are nearly identical, indicating the chemical uniformity of the polymer. However, a slightly broader peak was observed from the UV detector, which is possibly related to the absorption phenomena rather than size exclusion.[29] It is possible that minute fractions of unreacted precursor may be present, and this small fraction is extremely difficult to remove due to the similar characteristics of both polymeric systems. We believe that the aggregation behavior of this C_{60} containing copolymer in water will not be significantly altered due to the amphiphilic characteristics of the precursors.

The weight percentage of C_{60} in the P(*t*BMA-*b*-DMAEMA)-*b*-C_{60} polymer was determined by thermogravimetric analysis (TGA). The relative amounts of C_{60} and P(*t*BMA-*b*-DMAEMA) in the final copolymer were calculated by comparing its TGA curve with those of pure C_{60} and P(*t*BMA-*b*-DMAEMA) since the C_{60} is stable above 600 °C. The molar ratio of C_{60} to P(*t*BMA-*b*-DMAEMA) determined from TGA was close to 1:1, indicating that each polymer chain was end-capped to only one C_{60}.[13]

Finally, the *t*-butyl groups of the P(*t*BMA) blocks were hydrolyzed to form PMAA blocks. The fully hydrolyzed final product was confirmed by FT-IR (KBr-pellet), where a broad peak at 3500 cm^{-1} is present and the sharp peaks corresponding to *t*-butyl group at 1393 and 1368 cm^{-1} disappeared.

Figure 3 shows the UV−vis absorption spectra of P(MAA-*b*-DMAEMA)-*b*-C_{60} in aqueous solution at 25 °C. At pH 3, the absorption spectra show the characteristic C_{60} peaks at 256, 330,

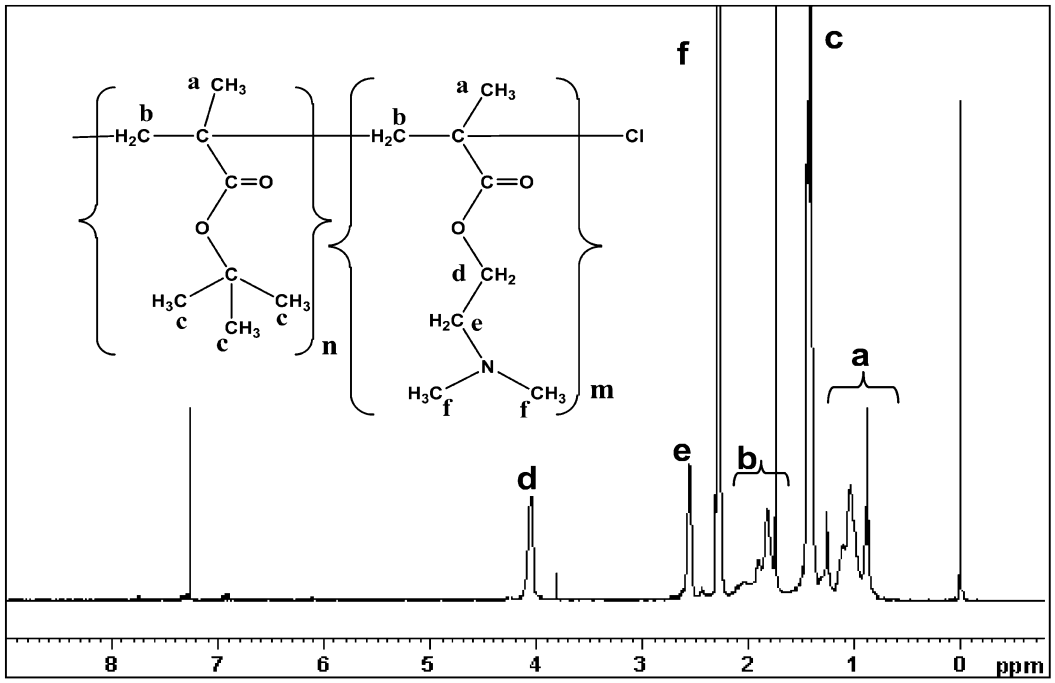

Figure 2. ^{1}H NMR spectrum of P(*t*BMA-*b*-DMAEMA) in $CDCl_3$.

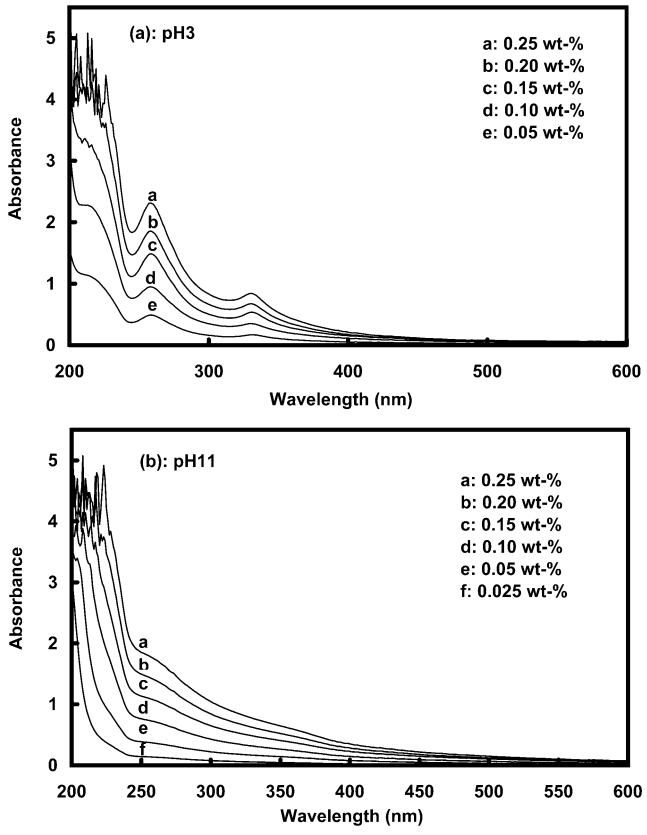

Figure 3. UV−vis spectroscopy of P(MAA_{102}-*b*-$DMAEMA_{67}$)-*b*-C_{60} in aqueous solutions at different pH values and concentrations.

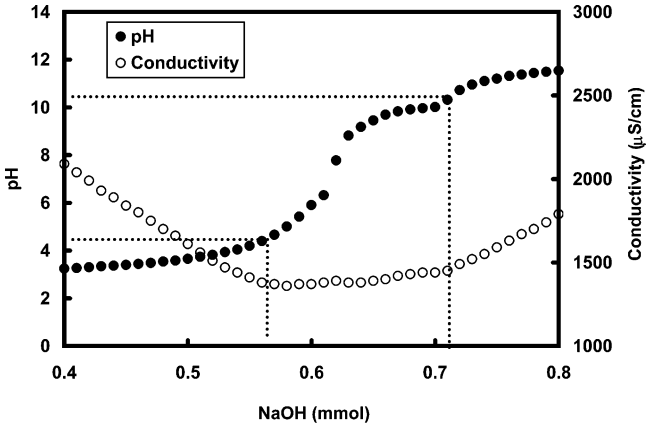

Figure 4. pH and conductivity titration curves of P(MAA_{102}-*b*-$DMAEMA_{67}$)-*b*-C_{60} at 25 °C and 1 atm.

and 400 nm. These suggest the successful grafting of the copolymer to C_{60} and are in agreement with the reported spectroscopic characteristics of mono-functionalized fullerenes in solution.[30,31] In contrast, the absorption spectra at pH 11 shows continuous absorption in the wavelength range of 200−500 nm. This may be attributed to the formation of the charge-transfer complex between the PDMAEMA segments and C_{60}, which perturbed the localization of the conjugated bonds.

The variation in absorption spectra with pH shows that the electronic environments around the C_{60} at pH 3 and 11 are different due to the disparity in aggregation phenomena. At 55 °C, the absorption spectra measured at pH 3 and 11 are similar to the corresponding spectra at 25 °C, indicating that the electronic environments around C_{60} has not been altered by the increase in temperature.

From the titration of 1 M NaOH into P(MAA-*b*-DMAEMA)-*b*-C_{60} aqueous solution at 25 °C, two transition points (pH ∼4.5 and ∼10.4) were observed from the pH and conductivity titration curves as shown in Figure 4. The first transition corresponds to the onset of neutralization of -COOH groups on the PMAA segments, and the second corresponds to the end of deprotonation of $-NH^+(CH_3)_2$ groups on the PDMAEMA segments. During the titration, it was observed that the clear solution turned cloudy at moderate pH and became clear again at high pH values. Visible light transmittance at a wavelength of 600 nm of P(MAA-*b*-DMAEMA)-*b*-C_{60} solution was measured from pH 2 to 12 to monitor the cloudy region as shown in Figure 5. It is evident that between pH 5.4 and 8.8, the copolymer becomes insoluble due to complexation and overall charge neutralization near the isoelectric point (IEP).[27,28] This behavior is similar to

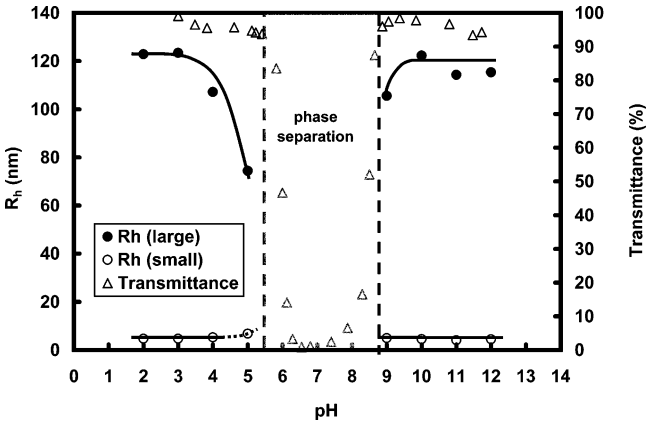

Figure 5. pH dependence of R_h and visible light transmittance at 25 °C.

that of P(MAA-*b*-DMAEMA)[28] and P(MAA-*b*-DEAEMA)[9] in solution. It can be concluded that the water-soluble C_{60} containing P(MAA-*b*-DMAEMA) retains the polyampholyte properties in solution. In addition, visible light transmittance of the solution measured at 55 °C shows that the pH of the insoluble region shifts slightly to between 5.2 and 8.4. This relative similarity of low- and high-temperature insoluble regimes is due to the intrinsic decrease of pH with increasing temperature and therefore indicates that the isoelectric point (IEP) of the copolymer is not drastically affected by changes in the temperature.

On the basis of the previous results, the stimuli-responsive behavior of the well-defined and water-soluble C_{60}-containing block copolymer in solution is demonstrated. Next, we examined the solution behavior of the copolymer with stepwise changes in pH for a complete understanding of pH-dependent association behavior in the soluble regions. Dynamic light scattering was carried out as a function of pH. The hydrodynamic radii were obtained by applying the Stokes−Einstein relationship to decay rates, and the pH dependence of the hydrodynamic radius (R_h) is shown in Figure 5. At pH values lower than 5 and higher than 9, decay time distribution functions revealed two translational diffusion modes, while at moderate pH phase separation occurs and no light scattering was carried out (experimental data from DLS are provided in Supporting Information). The average hydrodynamic radius of large particles remains constant at about 120 nm when the pH was increased from 2.0 to below 4.0. In this region, the PMAA segments are predominantly not dissociated because the pK_a of methacrylic acid (pK_a = 5.35) lies considerably above these pH values.[28] Similarly, the PDMAEMA segments are mostly protonated because the pK_b of PDMAEMA is at 8.00.[28] Therefore, it can be concluded that in this pH range, the copolymer microstructure is largely unaffected by variations in pH. The average hydrodynamic radius of large particles remained constant at about 120 nm when the pH was increased from 9.0 to 12.0, where the PMAA segments are primarily dissociated while the PDMAEMA segments are deprotonated. The copolymer microstructure in this pH range is also largely unaffected by pH change. We have therefore identified that the copolymer aggregation microstructure is, to a large degree, stable below and above the insoluble pH range and that the charge neutralization effects become significant only when the solution pH is close to the phase-separated range. In accordance with our hypothesis of stable microstructure over large pH ranges, the average size of small particles in the copolymer solution remains constant at 5 nm, which corresponds to monomeric polymer chains (or unimers). If the hydrophobicity of any segment changes or if electrostatic attraction becomes significant with changes in pH, unimers may cease to exist since they are maintained by the strong electrostatic repulsion between the positively charged chains, which keeps individual unimer chains solvated in aqueous solution. If the hydrophobicity of PDMAEMA increases significantly, the decrease in the hydrophile−lipophile balance (HLB) will favor the formation of micelles or larger aggregates. If electrostatic attraction between positively charged PDMAEMA and negatively charged ionized PMAA becomes significant, the formation of electrostatic complexes will produce insoluble precipitates. This will impede the formation of freely solvated unimers or cause a decrease in the size of aggregates.[27] The stability of unimer size is thus an indication of the stability of the copolymer microstructure.

In contrast to hydrodynamic radii stability below pH 4.0 and above pH 9.0, there is a slight drop in aggregate size at pH of ∼4.0 and ∼9.0 and a marked decrease near the insoluble range at pH 5.0. This phenomenon is attributed to the formation of charge complexes near this range as suggested by Gohy et al.[27] As the pH is increased to above 4.0, some of the MAA units are ionized, and they form complexes with positively charged PDMAEMA. These insoluble complexes form part of the hydrophobic core of the aggregates and cause a reduction in size. Indeed, the occurrence of local insoluble complexes arises within (and possibly near) the pH range 4.5−10.4.

On the basis of the previous findings for pH-dependent association behavior, we selected pH 3 and 11 to investigate the aggregation behavior of P(MAA-*b*-DMAEMA)-*b*-C_{60} as a function of temperature because these pH values represent stable conditions in the low and high-pH soluble ranges, respectively. The aggregation behavior of P(MAA-*b*-DMAEMA)-*b*-C_{60} at pH 3 was investigated using DLS at 25 and 55 °C. At this pH, the decay time distribution function revealed two translational diffusion modes, as is evident from the q^2 dependence of the decay rate. The fast decay mode corresponds to an average R_h of ∼5 nm, while the slow decay mode corresponds to an average R_h of ∼120 nm. The balance of hydrophobic attraction and electrostatic repulsion arising from positively charged amine groups, which accounts for the association of P(MAA-*b*-DMAEMA)-*b*-C_{60}, gives rise to the slow diffusional mode of the aggregates. The hydrophobic interactions arise from two different kinds of domains; the first consists of C_{60}, while the other comprises PMAA segments. Instead of forming simple core−shell-like micelles as in the diblock P(MAA-*b*-DMAEMA) system, the aggregates possess a microgel-like structure with hydrophobic domains composed of C_{60} and PMAA segments interconnected by charged hydrophilic PDMAEMA segments. The strong electrostatic repulsion also gives rise to the coexistence of unimers (fast decay mode) with these aggregates.

When the Stokes−Einstein relationship was applied to the decay time distribution at 55 °C, the hydrodynamic size distribution was nearly identical at both low and high temperatures. Large aggregates with an average radius of about 120 nm and unimers with an average radius of about 5 nm coexist in solution. This indicates that no apparent transformation in microstructure occurs with increasing temperature. At this pH, the PMAA segments and C_{60} molecules remain hydrophobic within the temperature range, while the PDMAEMA segments remain hydrophilic as they are fully protonated. In other words, the HLB of the copolymer is not adversely affected by the rise in temperature in this experimental range.

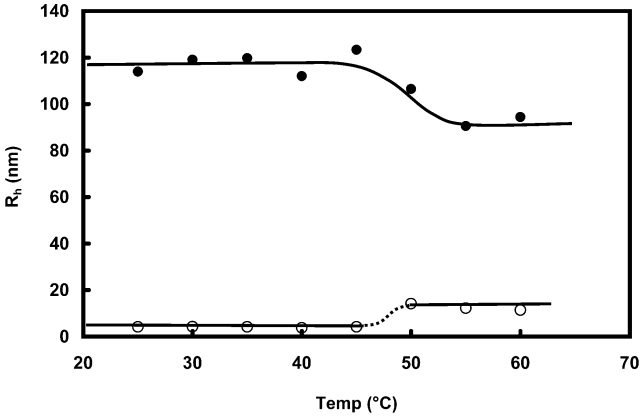

Figure 6. Temperature dependence of R_h values of P(MAA_{102}-*b*-$DMAEMA_{67}$)-*b*-C_{60} at pH 11.

At pH 11, the decay time distribution function also shows two translational diffusion modes at 25 °C. The fast mode corresponds to an average hydrodynamic radius of ~5 nm, while the slow mode corresponds to an average radius of ~120 nm. The ionized -COO^- and the deprotonated PDMAEMA segments are hydrophilic at this temperature, while the C_{60} is hydrophobic. Our previous work on PDMAEMA-*b*-C_{60} in aqueous solution at high pH revealed the formation of the charge-transfer complex between PDMAEMA segments and C_{60},[16] which enhanced the solubility of C_{60} in water. In the formation of this complex, the lone pair electrons on the nitrogen act as the electron donor, and C_{60} acts as the electron acceptor. Some of the C_{60} molecules aggregate with one another through hydrophobic interaction, while the others form the charge-transfer complex with PDMAEMA segments, and they act as physical cross-linkers. Therefore, large particles are produced in solution coexisting with unimers by the combination of hydrophobic interactions, electrostatic repulsion, and the charge-transfer interaction, which give rise to large aggregate complexes instead of simple core−shell-like micelles.

In contrast to the similarity of decay time distributions at pH 3, the difference in decay time distributions at 25 and 55 °C was apparent at pH 11. The temperature dependence of hydrodynamic radii is shown in Figure 6. A gradual shift in hydrodynamic size distribution occurred as the temperature was increased. Between 25 and 45 °C, unimers and aggregates coexist with no change in unimer or aggregate size. At 50 °C and beyond, an intermediate translational diffusion mode appears, corresponding to a hydrodynamic radius of about 13 nm while the fast mode disappears. The aggregates were smaller in size, with an average radius of only about 90 nm. The appearance of the intermediate mode, disappearance of the fast mode, and decrease in aggregate R_h all occur between 45 and 50 °C. As the temperature increases, hydrophilic PDMAEMA segments become hydrophobic.[28] Therefore, the C_{60} and PDMAEMA form a continuous hydrophobic domain at higher temperatures while PMAA is hydrophilic. This shift results in the tendency for micelle formation, with C_{60} and PDMAEMA comprising the hydrophobic core and ionized PMAA the hydrophilic shell. Whereas at low temperatures the hydrophilic PDMAEMA allows for unimer formation, the loss in hydrophilicity at higher temperatures causes micelles to form. The intermediate diffusion mode is thus attributed to micelles. Comparison with earlier studies on the properties of PDMAEMA and P(MAA-*b*-DMAEMA) block copolymers supports our hypothesis that the formation of micelles occur at elevated temperatures.[27] Lowe et al. found that the cloud point

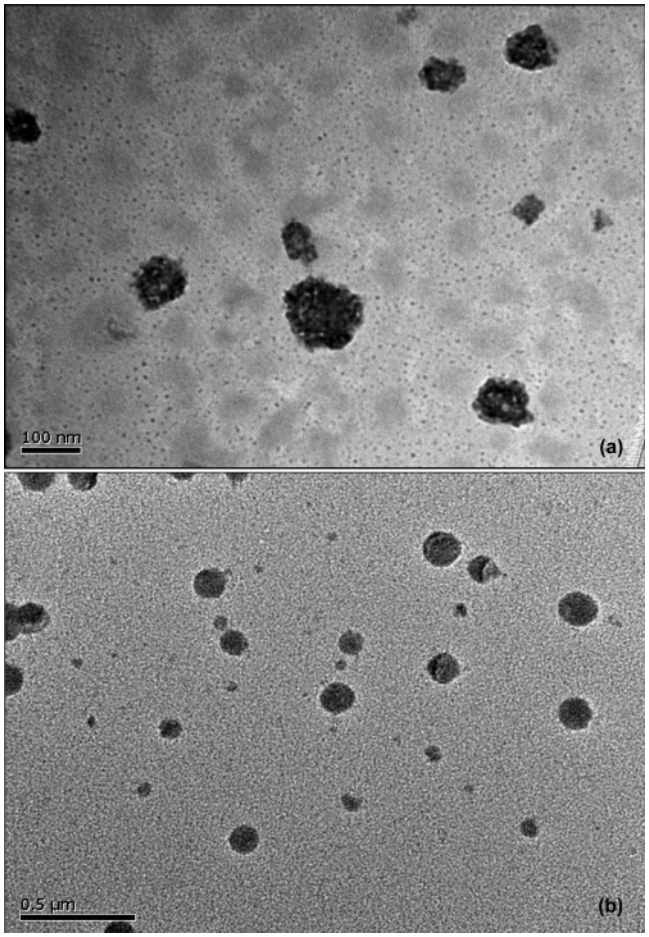

Figure 7. TEM images of P(MAA_{102}-*b*-$DMAEMA_{67}$)-*b*-C_{60} aggregates formed in aqueous solution at pH 3 (a) and pH 11 (b).

of a 1.0 w/v % PDMAEMA homopolymer solution at pH 9.5 is in the range of 32−46 °C depending on its molecular weight.[28] Therefore, at higher temperatures (in this case, at and above 50 °C), both C_{60} and PDMAEMA hydrophobicity induces the formation of core−shell micelles. The coexistence of aggregates with micelles suggests that at higher temperatures, the combination of charge-transfer and hydrophobic interactions control the formation of these aggregates. The decrease in size of the aggregates can also be explained by the diminishing hydrophilicity of PDMAEMA, which tends to minimize its interaction with water molecules, resulting in denser hydrophobic domains and thus a smaller aggregate size. The aggregates may also have larger aggregation numbers because of the decrease in HLB. The contribution to R_h from the increase in aggregation number is not as significant as the desolvation of PDMAEMA segments.

The TEM micrographs revealed large aggregates with porous cores at pH 3 and at 25 °C, as shown in Figure 7a. The cores of these aggregates are visibly less dense than those observed at pH 11 and at 25 °C (Figure 7b), which have compact cores. This indicates that the aggregate microstructures are different from each other.

A schematic representation of the aqueous microstructure of the copolymer is shown in Figure 8. Three contrasting microstructures were deduced across the pH and temperature ranges examined in the present study. At pH 3 and at 25 °C, unimers with positively charged PDMAEMA chains coexist with aggregates comprising separate C_{60} and PMAA hydrophobic domains. At pH 11 and at 25 °C, unimers with negatively charged ionized PMAA chains coexist with aggregates consist-

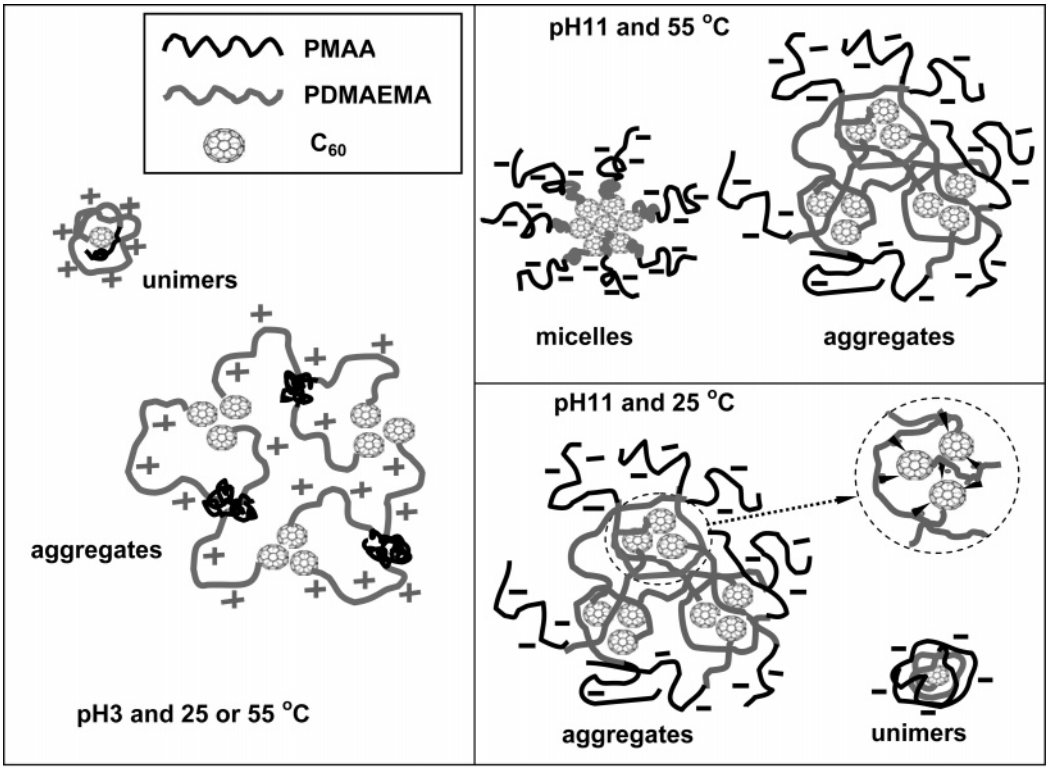

Figure 8. Schematic representation of the possible microstructures of P(MAA_{102}-*b*-$DMAEMA_{67}$)-*b*-C_{60} in aqueous solutions at different pH values and temperatures. The inset is the enlargement of the CT complex.

ing of C_{60} hydrophobic domains cross-linked due to charge-transfer interactions with PDMAEMA segments. The cross-linked cores proposed at this pH are compact cores of higher density than the porous cores hypothesized at pH 3. This is in agreement with the contrasting images visualized using the transmission electron microscope. At pH 11 and at 55 °C, micelles with a hydrophilic PMAA shell and a continuous hydrophobic C_{60} and PDMAEMA core coexist with aggregates of reduced size. The association behavior of the C_{60}-containing P(MAA-*b*-DMAEMA) copolymer contrasts with that of pure P(MAA-*b*-DMAEMA) of comparable composition. In the latter, smaller micelles and large hollow aggregates were formed below and above the IEP respectively at room temperature. The combination of electrostatic and hydrophobic interactions together with the minimization of chain-stretching of PDMAEMA blocks controls the formation of these large hollow aggregates.[27] In the C_{60}-containing block copolymer, the combination of electrostatic and hydrophobic interactions and the presence of C_{60} as an additional hydrophobic group as well as a charge-transfer acceptor produces unimers and aggregates at low pH and at high pH at low temperatures and micelles and aggregates at high pH and at high temperatures.

Conclusions

A well-defined and water-soluble C_{60}-containing ampholytic block copolymer was synthesized by ATRP, and its stimuli-responsive self-assembly behavior was systematically characterized by DLS and TEM. P(MAA_{102}-*b*-$DMAEMA_{67}$)-*b*-C_{60} showed enhanced solubility in aqueous medium at room and elevated temperatures at low and high pH but was insoluble at intermediate pH. The coexistence of unimers and aggregates was observed at low and high pH. At elevated temperatures at high pH, however, micelles and aggregates coexist. Hydrophobic and electrostatic interactions control the aggregate formation at low pH, while hydrophobic, electrostatic, and charge- transfer interactions control the aggregate formation at high pH. Although P(MAA_{102}-*b*-$DMAEMA_{67}$)-*b*-C_{60} possesses similar polyampholyte properties to P(MAA_{102}-*b*-$DMAEMA_{67}$), the aggregation mechanism is totally different from that of P(MAA_{102}-*b*-$DMAEMA_{67}$).

Acknowledgment. We thank Singapore-MIT Alliance for providing financial support.

Supporting Information Available: The decay time distribution functions of P(MAA_{102}-*b*-$DMAEMA_{67}$) in aqueous solutions at different measurement angles, pHs, and temperatures. This material is available free of charge via the Internet at http://pubs.acs.org.

References and Notes

(1) Nakamura, E.; Isobe, A. *Acc. Chem. Res.* **2003**, *36*, 807.
(2) Vinogradova, L. V.; Melenevskaya, E. Y.; Khachaturov, A. S.; Kever, E. E.; Litvinova, L. S.; Novokreshchenova, A. V.; Sushko, M. A.; Klenin, S. I.; Zgonnik, V. N. *Vysokomol. Soedin.* **1998**, *40*, 1854.
(3) Khonarev, D. V.; Lyubovskaya, R. N. *Uspekhi Khimii* **1999**, *68*, 23.
(4) Chiang, L. Y.; Bhonsle, J. B.; Wang, L.; Shu, S. F.; Chang, T. M.; Hwu, J. R. *Tetrahedron* **1996**, *52*, 4963.
(5) Brettreich, M.; Hirsch, A. *Tetrahedron Lett.* **1998**, *39*, 2731.
(6) Geckeler, K. E. *Trends Polym. Sci.* **1994**, *2*, 355.
(7) Yamago, S.; Tokuyama, H.; Nakamura, E.; Kikuchi, K.; Kananishi, S.; Sueki, K.; Nakahara, H.; Enomoto, S.; Ambe, F. *Chem. Biol.* **1995**, *2*, 385.
(8) Sun, Y. P.; Lawson, G. E.; Huang, W. J.; Wright, A. D.; Moton, D. K. *Macromolecules* **1999**, *32*, 8747.
(9) Dai, S.; Ravi, P.; Tam, K. C.; Mao, B. W.; Gan, L. H. *Langmuir* **2003**, *19*, 5175.
(10) Wang, X.; Goh, S. H.; Lu, Z. H.; Lee, S. Y.; Wu, C. *Macromolecules* **1999**, *32*, 2786.
(11) Song, T.; Dai, S.; Tam, K. C.; Lee, S. Y.; Goh, S. H. *Polymer* **2003**, *44*, 2529.
(12) Song, T.; Dai, S.; Tam, K. C.; Lee, S. Y.; Goh, S. H. *Langmuir* **2003**, *19*, 4798.

(13) Zhou, P.; Chen, G. Q.; Hong, H.; Du, F. S.; Li, Z. C.; Li, F. M. *Macromolecules* **2000**, *33*, 1948.
(14) Yang, J.; Li, L.; Wang, C. *Macromolecules* **2003**, *36*, 6060.
(15) Tan, C. H.; Ravi, P.; Dai, S.; Tam, K. C. *Langmuir* **2004**, *20*, 9901.
(16) Dai, S.; Ravi, P.; Tan, C. H.; Tam, K. C. *Langmuir* **2004**, 20, 8569.
(17) Liu, X. M.; Wang L. S. *Biomaterials* **2004**, *25*, 1929.
(18) Rackaitis, M.; Strawhecker, K.; Manias, E. *J. Polym. Sci., Part B: Polym. Phys.* **2002**, *40*, 2339.
(19) Kikuchi, A.; Okano, T. *Adv. Drug Deliv. Rev.* **2002**, *54*, 53.
(20) Saitoh, T.; Suzuki, Y.; Hiraide, M. *Anal. Sci.* **2002**, *18*, 203.
(21) Osada, Y.; Okuzaki, H.; Hori, H. *Nature* **1992**, *355*, 242.
(22) Roy, I.; Gupta, M. N. *Chem. Biol.* **2003**, *10*, 1161.
(23) Ma, Y. H.; Tang, Y. Q.; Billingham, N. C.; Armes, S. P.; Lewis, A. L. *Biomacromolecules* **2003**, *4*, 864.
(24) Tang, Y. Q.; Liu, S. Y.; Armes, S. P.; Billingham, N. C. *Biomacromolecules* **2003**, *4*, 1636.
(25) Wetering, P. v. d.; Cherng, J.-Y.; Talsma, H.; Hennink, W. E. *J. Controlled Release* **1997**, *49*, 59.
(26) Torres-Lugo, M.; García, M.; Record, R.; Peppas, N. A. *J. Controlled Release* **2002**, *80*, 197.
(27) Gohy, J.-F.; Creutz, S.; Garcia, M.; Mahltig, B.; Stamm, M.; Jérôme, R. *Macromolecules* **2000**, *33*, 6378.
(28) Lowe, A. B.; Billingham, N. C.; Armes, S. P. *Macromolecules* **1998**, *31*, 5991.
(29) Huang, X.; Goh, S. H.; Lee, S. Y. *Macromol. Chem. Phys.* **2000**, *201*, 2660.
(30) Bensasson, R. V.; Bienvenne, E.; Dellinger, M.; Leach, S.; Seta, P. *J. Phys. Chem.* **1994**, *98*, 3492.
(31) Guldi, D. M. *J. Phys. Chem. A* **1997**, *101*, 3895.